Biomedicine & Pharmacotherapy 109 (2019) 602–609

Contents lists available at ScienceDirect

Biomedicine & Pharmacotherapy

journal homepage: www.elsevier.com/locate/biopha

Atorvastatin alleviates early hypertensive renal damage in spontaneously hypertensive rats

Jiahui Zhao*, Qingli Cheng, Yang Liu, Guang Yang, Xiaohua Wang

Department of Geriatric Nephrology, Chinese PLA General Hospital, 100853, Beijing, China

ARTICLE INFO

Keywords:
Hypertension
Kidney damage
Atorvastatin
Inflammation

ABSTRACT

This study aimed to examine the effects of atorvastatin on early hypertensive renal damage and explored the underlying mechanisms. 12-week-old salt-loaded spontaneous hypertensive rats (SHRs) were divided into four groups: atorvastatin (AVT), losartan potassium (LP), atorvastatin combined with peroxisome proliferators-activated receptor γ (PPAR-γ) inhibitor (AVT + GW9662), and saline. During 10 weeks administration blood pressure and urea albumin creatinine ratio were determined. We also examined the renal function, pathological changes of kidney, inflammatory cytokines in the serum and the association of the change of inflammatory factors in the kidney tissue. AVT did not reduce the mortality of the SHRs. AVT reduced the blood pressure of SHRs, but the effect was not comparable to that of LP. AVT significantly decreased urine protein. AVT and LP displayed comparable effects by significantly decreasing inflammatory cytokines (hs-CRP, IL-1β, IL-6, TNF-α, and TGF-β) levels in serum. AVT and LP both apparently improved renal pathological changes and significantly reduced the infiltration of macrophage in renal tubular interstitial. Both mRNA and protein expression levels of TLR4, NFκB, MCP-1 were significantly down regulated in AVT and LP groups. There was no significant change in macrophage polarity. The addition of PPAR-γ inhibitor partially reduced the anti-inflammatory effect of AVT. These results mean that Atorvastatin can alleviates the pathology of hypertensive renal damage. Atorvastatin protects the kidney by reducing the apparent inflammation in salt-loaded SHRs. Atorvastatin alleviates inflammation partially by augmenting expression of PPAR-γ.

1. Introduction

Hypertension is a prominent public health issue worldwide and is a key risk factor for cardiovascular and kidney diseases. An epidemiological survey conducted in China in 2014 demonstrated that the prevalence of hypertension in adults over 18 years old was 25.2%. Hypertension causes a series of complications and is a major factor leading to chronic kidney disease (CKD). Hypertensive renal damage has a high prevalence and is a major cause of end-stage renal disease (ESRD), as studies demonstrated that 28% of ESRD cases were associated with hypertension [1,2]. The incidence of hypertension-mediated ESRD has been gradually increasing over the years [1,2]. However, with the exception of strict control of blood pressure, no effective clinical option for ESRD is available, indicating that early treatment of hypertensive renal damage is of vital importance. Atorvastatin is the most prescribed drug for treating hyperlipidemia, atherosclerosis, and coronary heart disease. Our previous studies have revealed that atorvastatin significantly alleviates the pathology of renal senescence by improving atherosclerosis and counteracting inflammation [3]. Hence, in this study, we examined the influence of atorvastatin on early hypertensive renal damage, thereby providing the experimental basis for developing new treatment of hypertensive renal damage.

2. Materrials and methods

2.1. Animal model and treatment groupings

All the 6-week-old spontaneous hypertensive rats (SHRs, purchased from Beijing Weitonglihua) were administered a high-salt diet (feed containing 8% NaCl) until the end of the experiment. After the rats reached 12 weeks old, they were administered different medications via gavage (once per day) along with a high-salt diet for 10 weeks until the rats were 22 weeks old. There were four interventions groups (n = 12), each containing equal numbers of male and female rats. The four groups were as follows: i) losartan potassium group (LP group), losartan potassium pills (a gift from Merck & Co.) were dissolved in saline and administered to rats at a dose of 20 mg/kg.d; ii) atorvastatin group (AVT group), atorvastatin pills (a gift from Pfizer) were dissolved in

* Corresponding author at: Department of Geriatric Nephrology, Chinese PLA General Hospital, 28, Fuxing Road, 100853, Beijing, China.
E-mail address: zjhpk301@163.com (J. Zhao).

https://doi.org/10.1016/j.biopha.2018.10.165
Received 20 June 2018; Received in revised form 26 October 2018; Accepted 26 October 2018

saline and administered at a dose of 10 mg/kg.d; iii) atorvastatin + peroxisome proliferators-activated receptor γ(PPAR-γ) inhibitor (GW9662) group (AVT + GW9662 group), atorvastatin pills and GW9662 (purchased from Sigma) co-dissolved in saline and administered at doses of 10 mg/kg.d atorvastatin and 0.5 mg/kg.d GW9662; and iv) normal saline group (control group), an equal volume of normal saline was administered. Rats were housed in the animal center of the Chinese People's Liberation Army (PLA) General Hospital. During the medication period, blood pressure was measured when rats were 12, 16, 20, and 22 weeks old; urine samples were collected to assess the urea albumin creatinine ratio (UACR, mg/mmol) when the rats were 12, 17, and 22 weeks old. Determination of blood pressure in rats by standard tail-cuff method (CODA Monitor, Kent Scientific corporation).

2.2. Collection of animal specimens

Urine samples were collected from the 22-week-old SHRs of the four experimental groups. The rats were then anesthetized (10% chloral hydrate) via abdominal injection and weighted. Three milliliters of orbital blood was extracted and centrifuged (2500rbm, 10 min) to obtain the serum (-80℃ conserve). An incision was introduced in the abdominal center before the two sides of the kidney were separated and weighted. The kidney was then quickly sliced into multiple portions. The lower right portion was fixed in 10% neutral buffered formalin, and the remaining tissues were stored in liquid nitrogen.

2.3. Determination of serum Scr, hs-CRP levels

The following serum parameters were tested: serum creatinine (Scr), blood urea nitrogen (BUN), total cholesterol (TC), triglycerides (TG), low-density lipoprotein cholesterol (LDL-C), high-density lipoprotein cholesterol (HDL-C), and hypersensitive-C-reactive protein (hs-CRP). The following urine parameters were tested: urine albumin creatinine ratio and urine N-acetyl beta-D glucosaminidase (NAG). All tests were performed on an automatic biomedical analyzer in the Department of Biochemistry, Chinses PLA General Hospital.

2.4. ELISA-based detection of inflammatory cytokines in the serum

Serum samples were isolated from the 22-week-old SHRs of the four experimental groups and analyzed using different kits (all purchased from eBioscience, include interleukin 1β (IL-1β), interleukin 6 (IL-6), tumor necrosis factor α (TNF-α), and transforming growth factor β (TGF-β)). Specifically, 100 μl protein standard and 100 μl sample were placed into the wells of a microtiter plate, incubated at 25 °C for 120 min and rinsed. 100 μl of biotin was added to each well, and the plates were then incubated at 25 °C for 60 min and rinsed. Subsequently, 100 μl HRP was added to each well, followed by incubation at 25 °C for 30 min and subsequent rinsing. 100 μl TMB substrate solution was then added into each well, and the plates were incubated at 25 °C in the dark for 15 min to facilitate color development. The reaction was terminated by adding 50 μl stop solution. The solutions were fully mixed for 30 min before OD values at 450 nm were measured. A standard curve was then plotted by placing OD values on the y-axis and concentrations of the protein standards on the x-axis. Correspondingly, the concentrations of individual samples were obtained based on their OD values and the standard curve.

2.5. Periodate-schiff (PAS) staining and Immunohistochemical analysis

After fixation in formalin, the samples were subjected to routine dehydration, clearing, paraffin embedding, and sectioning. The thin sections were then subjected to routine dewaxing and successive hematoxylin & eosin (HE) and periodate-schiff (PAS) staining. For immunohistochemical staining of CD68, paraffin sections were subjected to dewaxing, hydration, antigen retrieval, blockage of endogenous peroxidases, and blocking in 3% bovine serum albumin (BSA) at room temperature for 30 min. The slides were then probed with mouse anti-rat CD68 monoclonal antibody (Abcam) at 4 °C overnight before being rinsed and subsequently probed with HRP-conjugated goat anti-mouse secondary antibody (Jackson ImmunoResearch Laboratories) at room temperature for 50 min. The slides were rinsed and incubated with DAB substrate solution (brown indicates CD68 positive). The slides were then double stained with hematoxylin to reveal the nucleus before being dehydrated and sealed. CD68 expression was then semi-quantitatively assessed using microscopic image acquisition and analysis. Specifically, 20 high-magnification fields (400×) were randomly selected from each pathological section to enumerate positive cells, thereby calculating the count of positive cells of each group, which is expressed as the mean ± standard deviation. The degree of renal tubulointerstitial injury was scored according to the Katafuchi semi-quantitative criteria, including an assessment of renal interstitial inflammatory infiltration, renal interstitial fibrosis, and tubular atrophy [11]. The tubulointerstitial injury score was defined as follows: 0 (no injury), 1 (< 25%); 2 (25–50%); and 3 (> 50%).

2.6. Real-time PCR

The Tri^{zol} reagent (Invitrogen, Carlsbad, Calif., USA) Plus RNA Purification Kit was used to extract total RNA from the renal tissue of the four groups of 22-week-old SHRs. The concentration and purity of the RNA samples were determined after measuring absorbance values at 260 nm and 280 nm using a bioanalyzer. Then, the RNA concentration was adjusted to < 0.5 μg/10 μl. Reverse transcription was performed using a cycle of 70 °C for 5 min, 42 °C for 60 min, and 70 °C for 15 min. The resulting cDNA was mixed with primers (F/R) for the target genes (Table 1, synthesized by Taihe Biotechnology, Co. LTD.). Then, the amplification reaction was performed in a qPCR device with the following steps: 95 °C 5 min followed by 40 cycles of 95 °C 20 s and 60 °C 30 s. After amplification, the ΔCT values of the target gene and internal control GAPDH were compared to calculate the relative mRNA levels of the target genes. The target genes were toll like receptor 4(TLR 4), nuclear factor of kappa B (NFκBp65), monocyte chemoattractant protein-1(MCP-1), peroxisome proliferators-activated receptor γ (PPAR-γ), inducible nitric oxide synthase (iNOS), and arginase 1(Arg-1).

2.7. Western blotting

The kidney tissues of 22-week-old SHRs frozen in liquid nitrogen were retrieved. Total protein was extracted using precooled tissue

Table 1
The primer sequence of target gene.

gene	primer sequence (5'to3')
GAPDH	F : TGCTGAGTATGTCGTGGAG
	R : GTCTTCTGAGTGGCAGTGAT
iNOS	F : CAGCACAGAGGGCTCAAAGG
	R : CACATCGCCACAAACATAAAGG
Arg1	F : GCAGTGGCGTTGACCTTGT
	R : GCCTGGTTCTGTTCGGTTTG
PPAR γ	F : CTGCGTCCCCGCCTTAT
	R : TTCAATCGGATGGTTCTTCG
NF-κBp65	F : ATGGATCCCTGCACACCTTG
	R : CAAACCAAACAGCCTCACGG
MCP-1	F : GCCTGTTGTTCACAGTTGCT
	R : TGTAGTTCTCCAGCCGACTC
TLR-4	F : CCAGAGCCGTTGGTGTATCT
	R : AGAAGATGTGCCTCCCAGA

TLR4: toll like receptor 4; NF-κB: nuclear factor of kappa B; MCP-1: monocyte chemoattractant protein-1; iNOS: inducible nitric oxide synthase; Arg-1: arginase 1; PPAP-γ: peroxisome proliferators-activated receptor γ.

Table 2
Effects of medication on blood pressure in salt-loaded SHRs. MBP (mmHg, mean ± SD).

Group	12 w	16w	20w	22w	Change MBP (22w-12 w) / initial MBP (12 w) (%)	P
LP	174 ± 20	183 ± 16	172 ± 19	152 ± 22	−12.1 ± 11.3	< 0.05
AVT	174 ± 22	192 ± 25	174 ± 29	156 ± 29	−7.9 ± 7.1	< 0.05
AVT + GW9662	164 ± 26	183 ± 34	164 ± 29	147 ± 30	−5.7 ± 12.1	< 0.05
control	183 ± 35	195 ± 30	187 ± 42	205 ± 32	26.8 ± 11.3	

MBP: mean blood pressure ; AVT: atovastatin; LP: losartan potassium; GW9662: PPAR-γ inhibitor. P < 0.05, compared with the control group.

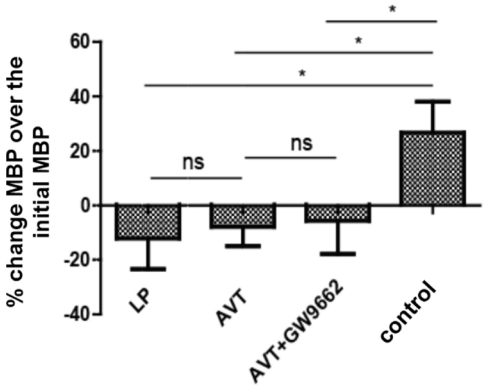

Fig. 1. Atorvastatin reduces the increase of blood pressure in salt-loaded SHRs. MBP: mean blood pressure, mmHg; AVT: atovastatin; LP: losartan potassium; GW9662: PPAR-γ inhibitor. ns, no significant, * p < 0.05, compared with the control group.

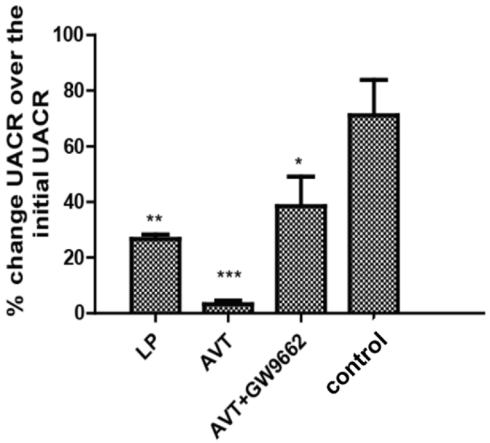

Fig. 2. Atorvastatin reduced the levels of urine protein in salt-loaded SHRs. UACR: urea albumin creatinine ratio, mg/mmol; AVT: atovastatin; LP: losartan potassium; GW9662: PPAR-γ inhibitor. * p < 0.05, ** p < 0.01, *** p < 0.001, compared with the control group.

Table 3
Atorvastatin improved the tubule interstitial lesions in SHRs. (mean ± SD).

Group	The score of renal tubule interstitial lesions	Scr(umol/L)	BUN(mmol/L)
LP	1.8 ± 0.9*	143 ± 13.6	10.0 ± 1.4
AVT	2.2 ± 1.0*	142.7 ± 10.7	9.7 ± 0.8
AVT + GW9662	3.9 ± 1.8	148 ± 8.0	10.1 ± 0.6
control	6.2 ± 2.3	144.3 ± 6.3	11.6 ± 1.6

AVT: atovastatin; LP: losartan potassium; GW9662: PPAR-γ inhibitor. * p < 0.05, compared with the control group.

lysate buffer. Protein concentrations were determined using the BCA Protein Assay Kit. Equal amounts of proteins from individual samples were denatured by mixing with loading buffer. The proteins were then

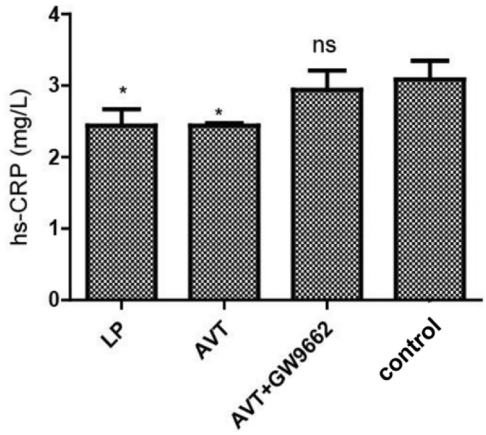

Fig. 3. Atorvastatin reduced the levels of hs-CRP (mg/L) in the salt-loaded SHRs.
AVT: atovastatin; LP: losartan potassium; GW9662: PPAR-γ inhibitor. ns, no significant, * p < 0.05, compared with the control group.

separated by SDS-PAGE and then transferred onto a nitrocellulose membrane. The membrane was blocked, probed with a primary antibody (all purchased from Abcam) against TLR4, NFκBp65, MCP-1, PPAR-γ, iNOS, and Arg-1 via incubation at 4 °C overnight, rinsed, probed with the corresponding secondary antibody (room temperature, 1 h), and rinsed again. Then, the membranes were subjected to enhanced chemiluminescence (ECL) color development and exposed to X-ray film. Densitometry analysis was then performed using IPP6 software to quantitatively determine the protein levels, and β-Actin served as the reference. The ratio of control/β-Actin was set at 1, and the ratio of target protein /β-Actin was calculated accordingly and used to represent the relative expression of this protein.

2.8. Statistical analyses

The measurement data are expressed as the mean ± standard deviation ($\bar{x} \pm s$). Then, a *t* test was performed to compare measurement data between two groups, and an *F* test was performed for comparison between more than two groups. In addition, a chi-square test, Fisher exact test and variance analysis were used to analyze inter-group differences. Statistical analyses were performed using SPSS 16.0 software. P < 0.05 was considered significant.

3. Results

3.1. The effect of atorvastatin on mortality in salt-loaded SHRs

When the rats were 22 weeks old, all rats of the losartan potassium group survived. In contrast, four rats of the atorvastatin group died (the remaining eight survived), yielding a mortality rate of 33%. Two rats of the atorvastatin + GW9662 group died (the remaining 10 survived), yielding a mortality rate of 16.7%. In the control group, six rats died, yielding a mortality rate of 50%. Although atorvastatin appeared to reduce the mortality in salt-loaded SHRs, the differences were not statistically significant. There was no statistically significant difference in

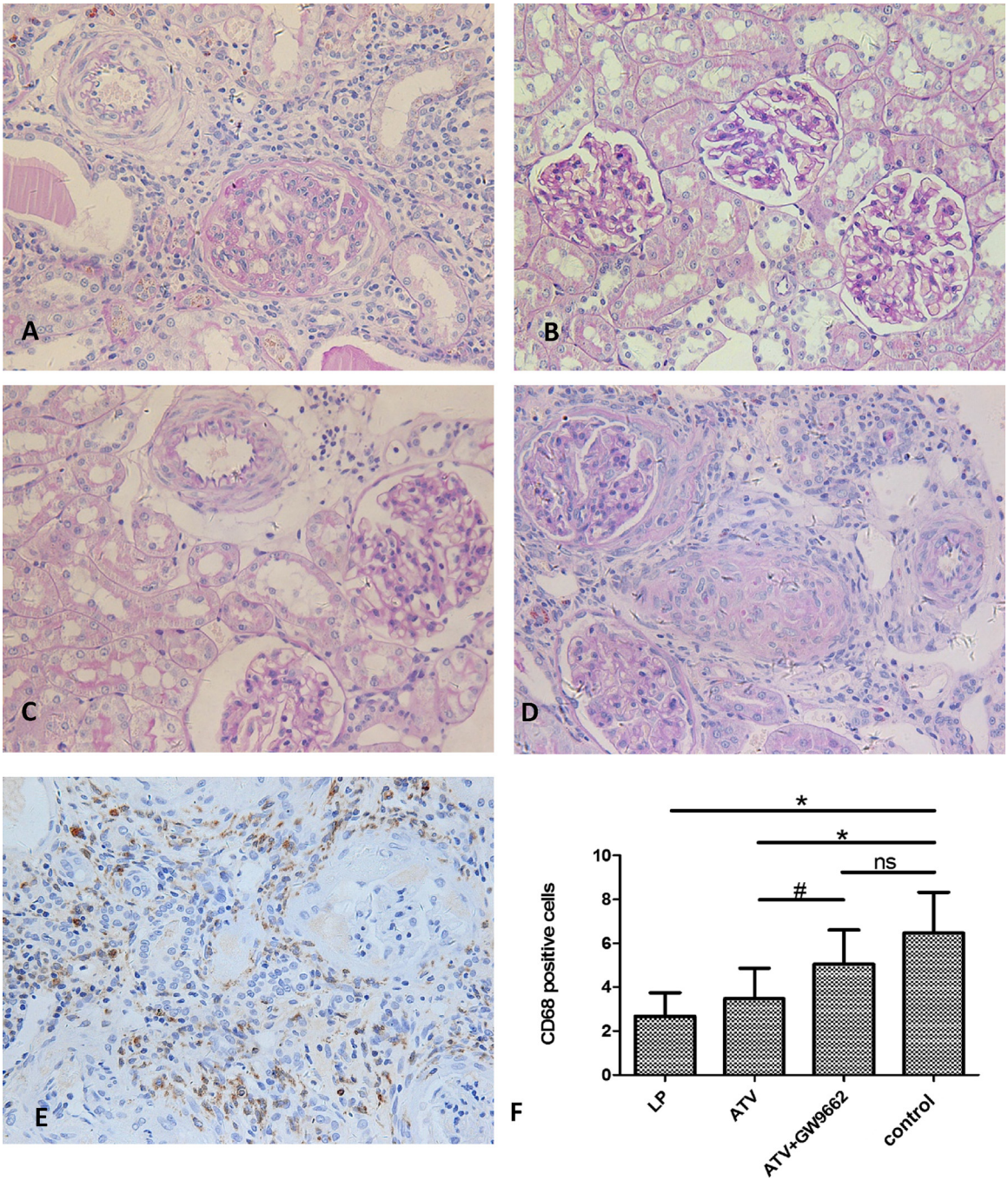

Fig. 4. Effects of atorvastatin on the renal pathology in 22 weeks old salt-loaded SHRs(PAS 400×)A : control ; **B** : LP ; **C** : AVT ; **D** : AVT + GW9662; **E** : CD68 immunohistochemical staining in the control group (400×); **F**: Atorvastatin decreased the CD68 positive cells. AVT: atovastatin; LP: losartan potassium; GW9662: PPAR-γ inhibitor. ns, no significant,* $p < 0.05$, compared with the control group. # $p < 0.05$, compared with the AVT + GW9662 group.

mortality between the groups

3.2. Atorvastatin decreased blood pressure in salt-loaded SHRs

A comparison between the atorvastatin and control groups revealed that the medication significantly reduced the blood pressure of salt-loaded SHRs ($P < 0.05$). The level of reduction was less than that of losartan potassium, but no significant differences were noted (Table 2, Fig. 1). Concurrent administration of PPAR-γ inhibitor did not significantly affect the atorvastatin-dependent antihypertensive outcome.

3.3. Atorvastatin significantly decreased urine protein levels in salt-loaded SHR

Both atorvastatin ($P < 0.001$) and losartan potassium ($P < 0.01$) significantly decreased urine protein levels in SHRs subjected to high salt intake, and the former displayed a superior outcome compared with the latter. However, the atorvastatin-mediated effect was apparently suppressed by concurrent administration of a PPAR-γ inhibitor, although the atorvastatin + GW9662 treatment reduced urine protein levels compared with the control ($P < 0.05$, Fig. 2).

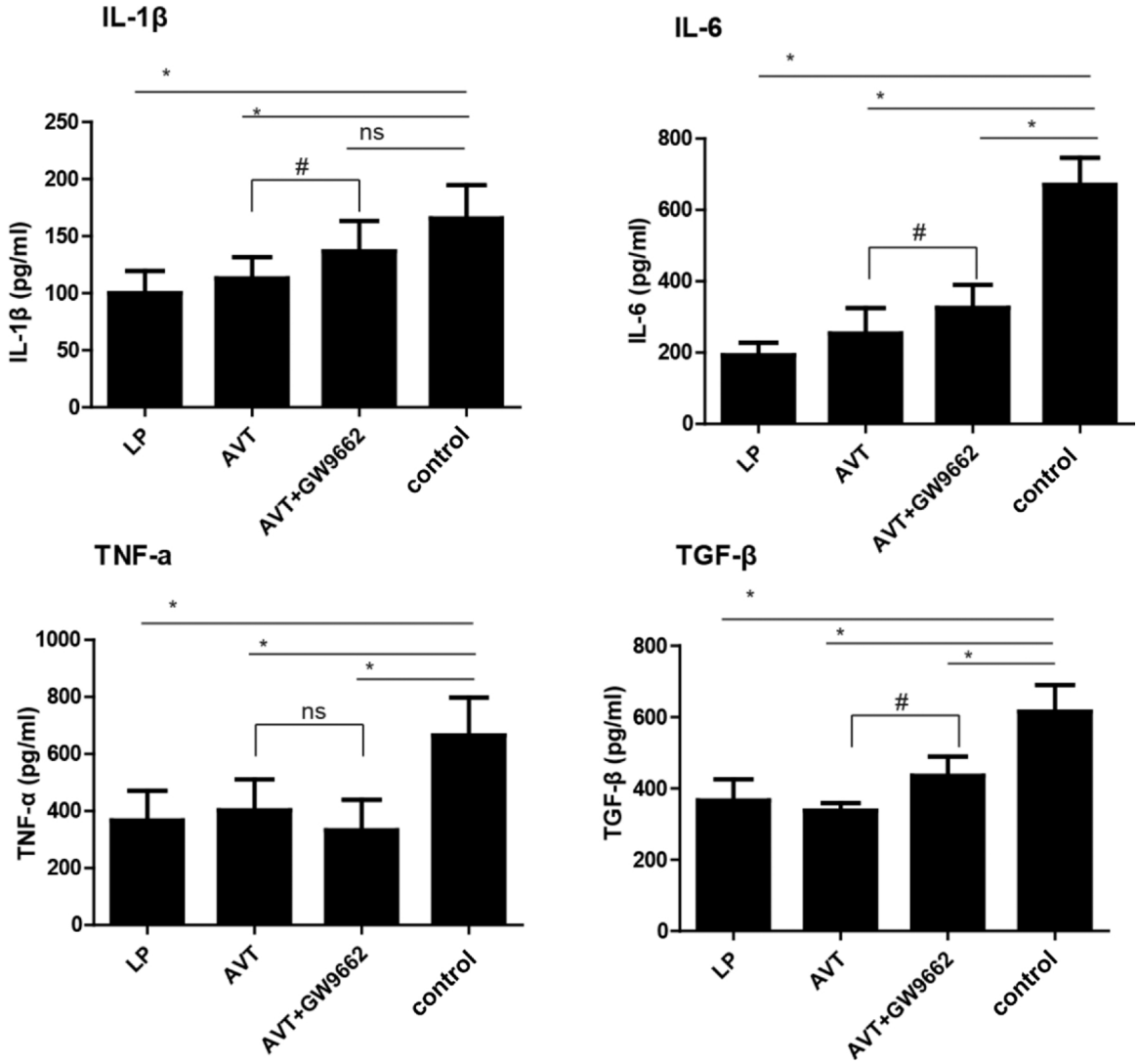

Fig. 5. Atorvastatin reduced the inflammatory cytokines in serum of 22 weeks old salt-loaded SHRs. Each bar represents the mean ± SD (n = 12). AVT: atovastatin; LP: losartan potassium; GW9662: PPAR-γ inhibitor; IL-1β: interleukin 1β; IL-6: interleukin 6; TNF-α: tumor necrosis factor α; TGF-β: transforming growth factorβ1. ns, no significant,* $p < 0.05$, compared with the control group. # $p < 0.05$, compared with the AVT + GW9662 group.

3.4. Atorvastatin did not appreciably alter renal function in salt-loaded SHRs

Rats from all four groups did not exhibit any prominent changes in blood lipid indicators. Specifically, administration of either atorvastatin or losartan potassium did not result in significant changes in renal functional indicators, including serum creatinine, urea nitrogen (Table 3), and urine NAG. However, both atorvastatin ($P < 0.05$) and losartan potassium ($P < 0.05$) significantly decreased hs-CRP levels in blood (Fig. 3).

3.5. Atorvastatin alleviated early hypertensive renal damage-induced pathological alterations and decreased macrophage infiltration in kidney of the salt-loaded SHRs

The renal pathological changes of 22-week-old SHRs under high salt intake included the following: minor proliferation of glomerular endothelial cells, ischemic changes in some glomeruli, shrinkage or collapse of loops of a few glomerular capillaries, intermediate level of inflammatory cell infiltration in renal tubular interstitium (more pronounced around arterioles), atrophy of a few tubules, no renal interstitial fibrosis, intima thickening on arteriole wall, and vascular stenosis (some vessels displaying hardening and even vascular occlusion, Fig. 4A). Both atorvastatin and losartan potassium clearly improved the aforementioned pathological changes in the 22-week-old SHRs, which displayed no apparent thickening of the arteriole wall, normal vascular lumen, no stenosis, normal glomeruli, no apparent endothelial cell proliferation, infiltration of very few inflammatory cells in the renal tubular interstitium, and no tubular atrophy or interstitial fibrosis (Fig. 4(B), (C)) and significantly reduced the score of renal tubule interstitial lesions(Table 3). After concurrent administration of a PPAR-γ inhibitor, atorvastatin-dependent improvements in renal pathology were slightly reduced (Fig. 4D). Semi-quantitative determination of CD68 revealed that both atorvastatin ($P < 0.05$) and losartan potassium ($P < 0.05$) significantly decreased macrophage infiltration in the renal tissues of rats and that the two drugs displayed comparable outcomes (Fig. 4 (E), (F)). After concurrent administration of a PPAR-γ inhibitor, macrophage infiltration in the renal tissues of the rats was mildly reduced but was no significantly different compared with the control group.

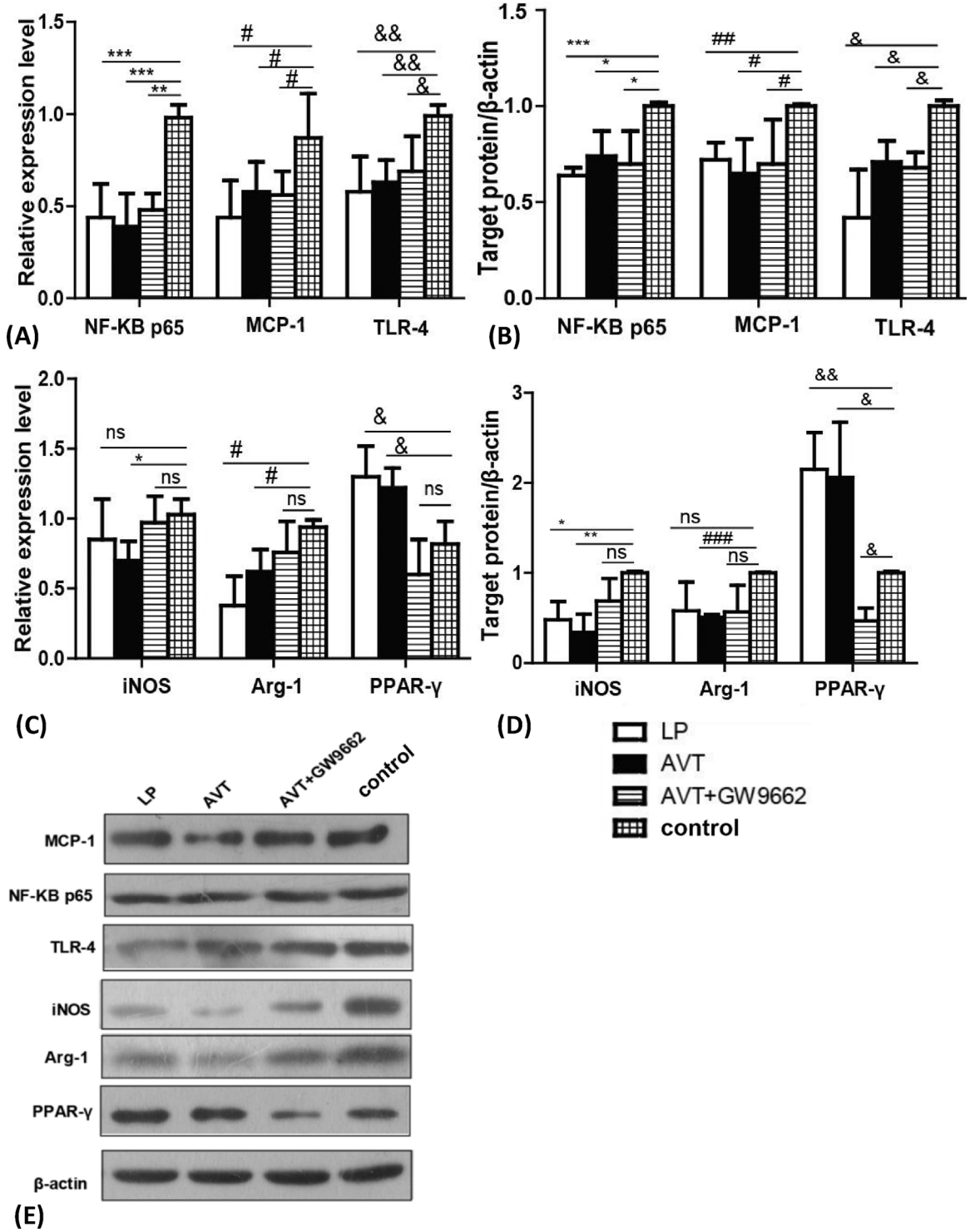

Fig. 6. Effects of atorvastatin on inflammatory markers expression in 22 weeks old salt-loaded SHRs. The protein (**E**) levels of TLR4、NF-κB p65、MCP-1、iNOS、Arg-1 、PPAP-γ in the kidneys; Quantities for densitometric analysis of mRNA (**A**、**C**) or protein (**B**、**D**). Each bar represents the mean ± SD(n = 12). AVT: atovastatin; LP: losartan potassium; GW9662: PPAR-γ inhibitor. TLR4: toll like receptor 4; NF-κB: nuclear factor of kappa B; MCP-1: monocyte chemoattractant protein-1; iNOS: inducible nitric oxide synthase; Arg-1: arginase 1; PPAP-γ: peroxisome proliferators-activated receptor γ. ns, no significant, * < 0.05, ** < 0.01, *** < 0.001; # < 0.05; & < 0.05, && < 0.01, compared with the control group.

3.6. Atorvastatin significantly decreased inflammatory cytokines in the serum of salt-loaded SHRs

Compared with the control, atorvastatin significantly decreased serum IL-1β, IL-6, TNF-α, and TGF-β concentrations, and the reduction levels were similar to those of the losartan potassium group (Fig. 5). Concurrent administration of a PPAR-γ inhibitor slightly diminished the atorvastatin-dependent reduction of inflammatory cytokines in serum.

3.7. Atorvastatin significantly reduced TLR4, NF-κB, MCP-1, iNOS, and Arg-1 levels in the kidney tissue of salt-loaded SHRs concurrently increased PPAR-γ expression

Real-time qPCR revealed that atorvastatin significantly reduced NF-κB p65, MCP-1, and TLR-4 mRNA levels in the kidney tissue of SHRs under high salt intake and that the outcome was comparable to that of losartan potassium (Fig. 6A). This result was further corroborated at the protein level by Western blot (Fig. 6B). However, iNOS, a biomarker of proinflammatory M1 macrophage, and Arg-1, a biomarker of anti-inflammatory M2 macrophage, were significantly reduced after atorvastatin and losartan potassium treatment. Atorvastatin induced increased PPAR-γ expression in the renal tissue of SHRs, and the outcome was comparable to that of losartan potassium treatment. Concurrent administration of PPAR-γ inhibitor did not significantly alter atorvastatin-dependent reductions in NF-κB, MCP-1, and TLR-4 expression but slightly diminished reduced Arg-1 and iNOS expression (Fig. 6(C), (D)).

4. Discussion

Inflammation was recently identified as the key factor contributing to the persistent progression of hypertensive renal damage [4,5]. In this study, salt-loaded SHRs at a very young age developed hypertension and proteinuria and began to die when they were 22 weeks old. The renal pathological manifestations included damaged glomerular endothelial cells, ischemic changes in some glomeruli, intermediate level of inflammatory cell infiltration in renal tubular interstitium, low levels of tubular lesions and vascular stenosis, but no interstitial fibrosis. Studies have demonstrated that hypertensive renal damage mostly comprised injury in multiple types of endothelial cells and infiltration of inflammatory cells. We reasoned that protracted hemodynamic abnormalities cause injury in endothelial cells, which subsequently activate inflammation system. As a consequence, massive macrophage infiltration occurs in the renal interstitium, where various inflammatory cytokines are highly expressed. Finally, the kidney enters a chronic inflammatory state that triggers severe, protracted kidney damage. This theory is consistent with most relevant studies. Although the renal lesions in the SHRs were not sufficient to cause death and serum creatinine levels were within in a normal range, the rats displayed a marked increase in mortality. We hypothesize that this effect was associated with severe hypertension-induced cerebrovascular diseases. Long-term administration of atorvastatin in SHRs significantly decreased proteinuria severity, decreased blood pressure, and improved early hypertensive renal damage-induced renal pathology. Hence, our results revealed that atorvastatin displayed comparable efficacy as losartan potassium in improving the renal functions of the SHRs.

Losartan potassium is a well-known angiotensin receptor blocker that is capable of abrogating activities of renin–angiotensin–aldosterone system (RAAS), thereby protecting endothelial cells and alleviating inflammation. However, the therapeutic efficacy of atorvastatin for early hypertensive renal damage was almost on par with losartan potassium. In recent years, atorvastatin has become the most widely prescribed lipid-lowering drug and is currently used by over 200 million cardiovascular patients. Studies have demonstrated that atorvastatin displays effects including influencing cell signaling and cell proliferation and inhibiting inflammation [6,7]. The SHRs model employed in this study exhibits normal blood lipid levels, thus excluding the possibility that blood lipid levels might affect the medication outcome. Our results revealed that atorvastatin displayed comparable performance as losartan potassium in suppressing inflammation in SHRs, as manifested by reduced levels of inflammatory cytokines, including IL-1β, IL-6, TNF-α, TGF-β, and hs-CRP in blood and TLR4, NF-κB, and MCP-1 in the kidney. In addition, the medication significantly decreased macrophage infiltration in tubule interstitium. It is speculated that atorvastatin can lower blood pressure slightly,which is related to improving vascular endothelial function and alleviating vascular sclerosis. It was speculated that atorvastatin can alleviat the pathologic damage in SHRs might be caused by protecting endothelial cells, reducing inflammatory response, reducing the degree of hardening of blood vessels at all levels in the kidney and reducing chronic and persistent renal ischemia. In recent years, there have been many studies on atorvastatin to inhibit inflammatory response. One possibility is that statins, which are selective inhibitors of 3-hydroxy-3-methylglutaryl CoA reductase inhibit receptor-G protein coupled signaling, for example, angiotensin II stimulated pathways by affecting G protein isoprenylation. It could also affect other signaling pathways that are also dependent on G proteins, e.g., chemokine receptor signaling pathways that are important in macrophage accumulation, NF-kB activation etc. [8]. Our study mainly discussed the effect of atorvastatin on PPAR-γ. Our data revealed that both atorvastatin and losartan potassium increased PPAR-γ expression. Although atorvastatin still exhibited inflammation inhibition when high PPAR-γ expression is abrogated, the anti-inflammatory outcome was diminished. Similarly, atorvastatin improved ventricular hypertrophy and augmented diastolic function in elderly SHRs by suppressing inflammatory cytokines [9]. In monocytes, atorvastatin activated the PPAR-γ pathway to suppress inflammation [10]. Finally, our results also demonstrated that the atorvastatin-dependent inhibition of inflammation could be slightly reduced by a PPAR-γ inhibitor, indicating that the anti-inflammatory activity is partially but not completely dependent on activation of the PPAR-γ pathway. In addition, the study also found that the treatment with atorvastatin and losartan potassium decreased the infiltration of the macrophages into the renal cortex, including the pro-inflammatory M1 and the anti-inflammatory M2, but ratio of M1 to M2 did not change remarkably. The polarity of macrophages did not change significantly after the two kind of drugs treatment.

In conclusion, we demonstrate that atorvastatin displayed comparable performance as losartan potassium in suppressing inflammation and significantly alleviate the pathology of early hypertensive renal damage and that the anti-inflammatory activity is partially dependent on activation of the PPAR-γ pathway. These results suggest that the multi-target, combined regimen of atorvastatin and losartan potassium may offer significant therapeutic benefit if applied to hypertension patients.

Conflict of interest

We declare that the authors have no competing interests.

References

[1] K. Reynolds, D.F. Gu, P. Muntner, J.W. Kusek, J. Chen, X.G. Wu, X.F. Duan, C.S. Chen, M.J. Klag, P.K. Whelton, J.A. He, et al., Population-based, prospective study of blood pressure and risk for end-stage renal disease in China, J. Am. Soc. Nephrol. 18 (6) (2007) 1928–1935.
[2] W. Zhang, W. Shi, Z.S. Liu, Y. Gu, Q. Chen, W.J. Yuan, et al., A nationwide cross-sectional survey on prevalence, management and pharmacoepidemiology patterns on hypertension in Chinese patients with chronic kidney disease, Sci. Rep. 20 (6) (2016) 38768.
[3] J.H. Zhao, Q.L. Cheng, P. Ye, G. Yang, S. Liu, Q.G. Ao, et al., Atorvastatin improves pathological changes in the aged kidney by upregulating peroxisome proliferator-activated receptor expression and reducing matrix metalloproteinase-9 and transforming growth factor-β1 levels, Exp. Gerontol. 74 (2) (2016) 37–42.
[4] S. Mennuni, S. Rubattu, G. Pierelli, G. Tocci, C. Fofi, M. Volpe, Hypertension and kidneys: unraveling complex molecular mechanisms underlying hypertensive renal damage, J. Hum. Hypertens. 28 (2) (2014) 74–79.
[5] J. Cui, J. Wan, D. You, Z. Zou, Y. Chen, Z. Li, et al., Interstitial complement C3 activation and macrophage infiltration in patients with hypertensive nephropathy, Clin. Nephrol. 88 (12) (2017) 328–337.
[6] E. van der Meij, G.G. Koning, P.W. Vriens, M.F. Peeters, C.A. Meijer, K.E. Kortekaas, et al., A clinical evaluation of statin pleiotropy: statins selectively and dose-dependently reduce vascular inflammation, PLoS One 8 (1) (2013) e53882.
[7] A. Oesterle, U. Laufs, J.K. Liao, Pleiotropic effects of statins on the cardiovascular system, Circ. Res. 120 (1) (2017) 229–243.
[8] A. Cai, Y. Zhou, L. Li, Rho-GTPase and atherosclerosis: pleiotropic effects of statins, J. Am. Heart Assoc. 4 (June(7)) (2015).
[9] J. Lu, F. Liu, F. Chen, Y. Jin, H. Chen, D. Liu, et al., Amlodipine and atorvastatin improve ventricular hypertrophy and diastolic function via inhibiting TNF-α, IL-1β

and NF-κB inflammatory cytokine networks in elderly spontaneously hypertensive rats, Biomed. Pharmacother. 83 (2016) 330–339.

[10] O. Grip, S. Janciauskiene, S. Lindgren, Atorvastatin activates PPAR-gamma and attenuates the inflammatory response in human monocytes, Inflamm. Res. 51 (2) (2002) 58–62.

[11] R. Katafuchi, Y. Kiyoshi, Y. Oh, N. Uesugi, K. Ikeda, T. Yanase, Fujimi S.GLomerular score as a prognosticator in lgA nephropathy : its usefulness and limitation, C1in Nephrol 49 (1) (1998) 1–8.